A98-31552

ICAS-98-3,6,2

EFFECTS OF USING BI–FLAP–SYSTEM ON THE IMPROVEMENT OF ARODYNAMICS OF A SWEPTBACK WING①

Ding–Ding Xin
(Ting–Ding Hsing)
Institute of Fluid Mechanics, Beijing University of Aeronautics
and Astronautics, Beijing 100083, P.R.China

Li Yuan
Institute of Mechanics, Chinese Academy of Sciences,
Beijing 100080, P.R.China

Abstract. The bi–flap–system is a device comprising an apex–flap and leading– edge–flaps located on the forepart and after part of a 74 ° delta wing respectively in this study. Through controlling the vortex separated from the leading–edge–flaps by that from the apex–flap, the aerodynamic characteristics of the wing can be improved on enhancing the ability of reducing drag ,increase of lift–drag ratio and the improvement of the nature of wing stall. This concept of vortex–control is based on using double vortex system in dominating the flow past wing, which differs from that by using single vortex like the wing–strake and vortex–flap. The superiority of using bi–flap–system to others and its principle of vortex control are interpreted in this paper through comparisons among exprimental results which were verified by the numerical solution of the Navier–Stokes equations with the turbulent effect preliminarily considered at $Re = 1x10^6$. According to our former investigations, the bi–flap–system is effective even at high speed up to Mach no.= 2.0 and in the case of wing–body combination.

Introduction

The flow past highly sweptback wings mounted on high speed aircrafts generally separates at the leading–edge and rolls up into two large vortices over the wing, which will induce an additional normal force or lift at the cost of some drag reduction due to the loss of leading–edge suction resulted from the flow separation (fig.1a). Therefore, besides the increase of lift, much attention has been paid since early seventies on how to suppress the drag rise. Afterwards there appear devices capable of controlling the flow field for reducing drag, such as the leading–edge projection, wing slots[1] etc..In general, they were developed under the principle of dominating the flow by controlling a single vortex system. Round about the year of 1980, the concept of vortex–flap attached to the leading–edge of sweptback wing was proposed by the scholars[2][3] in NASA. It was to droop down the vortex–flaps for producing a forward inclined force exerting on the flap with its tangential component capable of compensating the drag–rise induced by seperation. Its concept of vortex control was also based on the control of single vortex system (fig.1b), which differs from the control by using two–vortex system as performed in the bi–flap–system case (fig.1c).

Since, besides the beneficial activity of the leading–edge vortex–flaps mentioned above, the down drooped apex–flap also possesses the ability of delaying the breakdown of main vortices over the wing and in turn to increase the critical angle of attack(AOA) α and the corresponding maximum lift (coefficient C_l) as described in our former papers[4][5][6] and recently by the scholars in Virginia Polytechnic Institute and State University[7]. Therefore it is promising as was confirmed in our former investigations to install both the apex–flap and leading–edge vortex–flaps on a same sweptback wing (a bi–flapped wing, i.e. a wing with bi–flap–system) as shown in Fig.2c,d. In this paper, the effect of using bi–flap–system and the physical idea concerning

①The project supported by National Natural Science Foundation of China under Contract 19393100 and National Aviational Science Foundation under Contract 9105A003B

21st ICAS Congress
13-18 September 1998
Melbourne, Australia

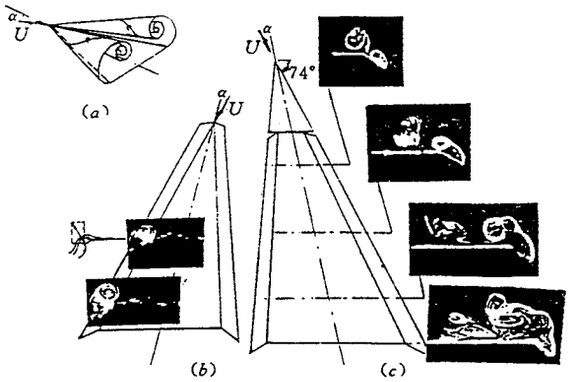

Fig.1 The Patterns of Flow past Various Sweptback Wings

(a) delta wing, (b) delta wing with rectangular vortex–flap(NASA), (c) delta wing with apex flap and leading–edge flaps(wing–1).

the control of vortical flow are considered. The bi–flap–system here considered is a device comprising an apex–flap (AF) and leading–edge–flaps (LEF) similar to the vortex–flap ofNASA pattern[2][8](Fig.2b). They are situated respectively on the forepart and after part of a 74 ° delta wing (Fig 2.a). Actually,the apex–flap is the foremost part of the delta–wing which can be deflected up and down about a transverse axis. The first vortex system is the vortex separated from the leading–edge of AF to interact with the second vortex system separated from the leading–edge of the LEF behind the AF. The interaction makes the first vortex system to merge with the second vortex system causing a change of load acting on LEF. The two models (Fig.2c,d) designed for the study of bi–flap system are different in form. The difference is in that one has its LEF located within the region of delta–wing, called WING–1[4][5](Fig.2c), which seems proper for missiles, while the other is to locate the LEF out of the main delta–wing, called WING–2[9][10](Fig.2d) which seems suitable for airplanes because of having larger aspect ratio and occupying less inner space within the main delta–wing.

In the following, the basic property of the flow past the wing and the principle of vortex control are explained followed by a comparison of the characteristics among wing with NASA patterned vortex–flap, the wing–1 and wing–2 under the control of bi–flap–system . Through comparison, the effects of using bi–flap– system on the improvement of the aerodynamics of sweptback wings can be understood.

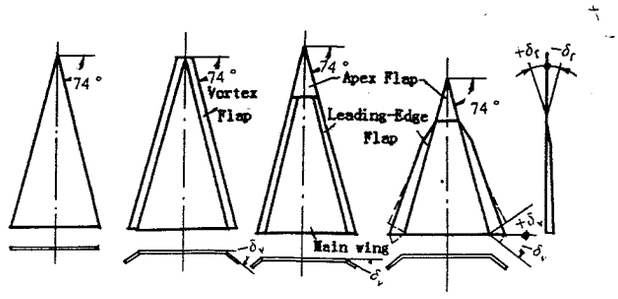

Fig.2 Wing Planforms

(a) delta wing, (b) wing with NASA patterned vortex–flap, (c) wing–1, (d) wing–2

Basic Characteristics of the Flow past Wing and the Principle of Vortex Control via Bi–Flap–System

Basic characteristics

In the case of bi–flapped wing, there are two effects that account for the downward drooped AF to have the ability of reducing the drag. The first is the direct effect resulted from the pressure acting on down drooped AF, which is inclined forward having a thrustwise component opposite to the drag. The second is an important effect indirectly resulted from the beneficial interaction of the two vortex–systems. In fact, one vortex–system separated from the down drooped AF having local angle of attack (AOA) less than that at the main delta wing is weaker and would be entrapped by the stronger vortex system separated from the LEF located behind. The more AF drooped down, the weaker the strength of the vortex separated from AF and the earlier the mergence will occur at a place nearer to the wing apex. This phenomenon can be observed clearly in the pictures taken from the flow visualization tests carried out in a 400 × 400 mm water channel at BUAA as shown in Fig.3a,b,and c. In these pictures the vortex merging points denoted by the arrows are to move towards the apex as the AF droops from 0 ° ,–10 ° to –20 ° for the wing–1 at $\alpha = 30$ ° . Correspondingly, a larger extent over the upper surface of LEF is covered by the combined vortex be-

xin

hind the merging point, which is conducive to the enhancement of the induced suction acting on LEF causing the total drag to reduce further. The latter effect can be testified again by the experimental

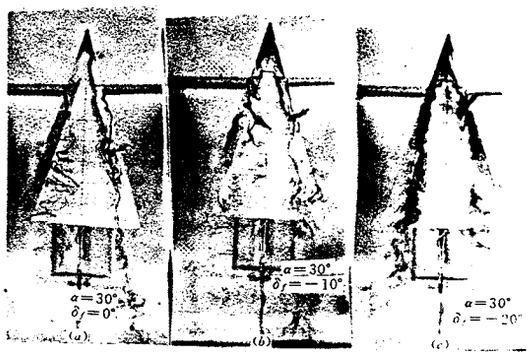

Fig.3 Vizualization Pictures with the Arrow Showing the Mergence Happened on the Leading–Edge Flap of Wing–1 at $\alpha = 30$ °
(a) $\delta_f = 0$ ° (b) $\delta_f = -10$ ° (c) $\delta_f = -20$ °

and computational results of the sectional load distribution shown in fig.4 for the wing–1. It can be seen that due to the greater extension of the area influenced by the merged vortex and the increase of strength of the vortex after mergence, the local load acting on the LEF region is increased as the AF deflects more downward (more nagative), while simultaneously the local load acting on the main delta–wing is to decrease, because the

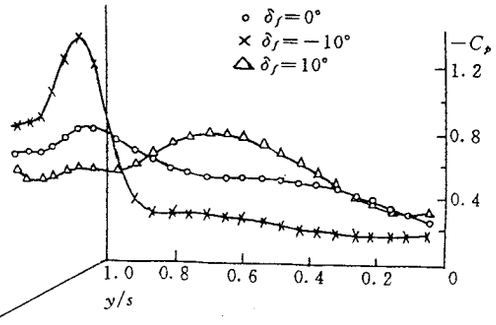

Fig.4 $\alpha = 15$ °, Spanwise Pressure Distribution of Wing–1 at 50% Chord (Cp––pressure coefficient, $y/s \leqq 1$––at main wing, $y/s \geqq 1$––at LEF)

increase of local flow–downwash will cause the local AOA and the local load to decrease at mian delta wing, which will in turn offset the increment of the local load acting on the AF to keep the total normal force of the whole wing nearly unchanged. On the contrary, opposite results will be obtained when the AF deflects upward. According to this explanation, other arodynamic characteristics of the bi–flapped wing such as the lift is only slightly less than the delta wing for AOA = 25 ° to 30 ° or below with no regards to whether the deflection of AF is downward or upward as can be seen from the curves of lift–coefficient C_l vs. AOA in Fig.5a. However for AOA greater than 30 ° the C_l will be greater especially in the case of downward drooped AF ($d_f < 0$)

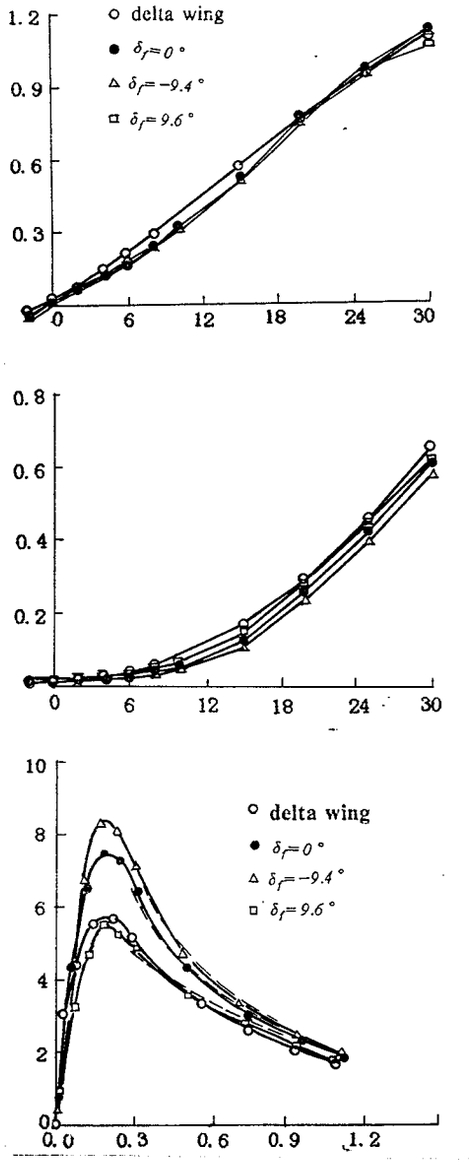

Fig.5 Characteristic Curves of Delta Wing and Wing–1 wth Various Apex–Flap Deflection (a) C_l–a, (b) C_d–a, (c) K–C_l.

xin

because of the delay of the vortex break–down. The curves in Fig.5b show the advantageous effect of using bi–flap system on improving the drag characteristics, where the drag coefficient C_d vs.AOA curves are drawn to indicate the reduction of C_d by drooping down the AF. In Fig.5c,

the corresponding lift–drag ratio $K = C_l / C_d$ vs. C_l for both the experimental and computational (by panel method[11]) results are drawn for comparison, which reveals the advantageous increase of K by using bi–flap–system on wing–1. Similar phenomeon is to occur in the case of wing–2 as to explain later.

Principle of vortex interaction under the control of bi–flap–system

The basic principle of the bi–flap–system used for controlling the vortices separated from sweptback wing is that a weak vortex would be entrapped by a stronger vortex and merges into a new single whole, as mentioned, if the interval between the two vortices is smaller than a certain critical value. According to the hydrodynamic study, the mergence of two rectiliner vortices with equal strength and rotating in same sense will take place if the nondimensional critical distance D / d equals about 1.7[12] is attained, where D and d are the interval between vortex centers and the diameter of vortex core respectively. Numerical investigations were also made in BUAA based on solving Navier–Stokes equations by using pseudo–spectral method to simulate the process of vortical mergence in 2–D and 3–D cases[13][14]. It was found, besides the mergence of a pair of equally strengthened vortices with D / d≦ca.1.7, there will be mergence for D / d larger than 1.7 at first but reduced to ca.1.7 afterwards due to the increase of vortex diameter d by diffusion. In addition, when D / d is less than the critical value, more severe stretch of the vortex will occur, which leads first to a quicker decrease of vorticity before the mergence and then followed by a more gradual slop of vorticity change after the mergence in comparison with those having D / d larger than the critical and without mergence as shown in Fig.6, where only the curve of D / d = 1.67 pertains to having mergence. Therefore, the total strength of the vortex after mergence is larger than those containing two isolated vortices without mergence as time goes on. The computation verified further that the stronger vortex always entraps the weaker one, causing a much stronger single vortex to appear after mergence just like that happened in the mergence of two vortices with equal strength.

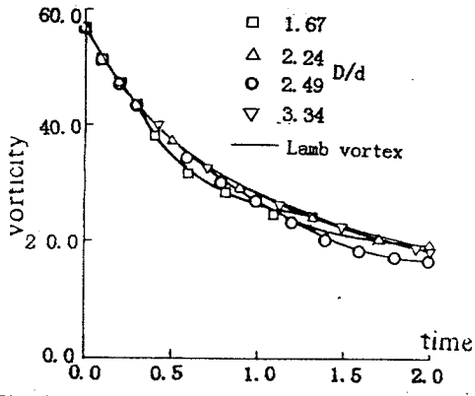

Fig.6 Decay of Vorticity at Vortex–Center for Two Vortices With Same Sence under the Action of Mergence (D = D / d)

Aerodynamic effect of the vortex control on delta wing with single–flap(after NASA) and bi–flap–system(wing–1)

Aerodynamic effect of the bi–flap–system on wing–1 and on the wing with NASA patterned LEF.

Most of the experimental results discussed below were obtained from the tests carried out in a low speed wind–tunnel at the Peking University having a circular test–section with diameter = 2.2 m. The experimental Reynolds no. was about 1×10^6 for all tests. For the delta wing with single leading–edge flap we used, was a 74 ° delta wing equipped with downward deflected LEF ($\delta_v = -30$ °) after the pattern of NASA, which is very effective on vortex control as can be found in NASA papers[2][8]. In Fig.7,the C_l–α and K–C_l characteristic curves are drawn for two wing–planforms with different n, which is the area ratio of AF to the wing, but with their LEF equally downward deflected to dv = −30 ° .Here the wing with n = 0 is the wing equipped with NASA pattered LEF but without AF, while n ≠ 0 is the wing–1, i.e. the bi–flapped wing with straight leading–edge and AF。 The AF is deflected downward to $\delta_f = -10$ ° . It can be seen that by

xin

drooping the AF, the lift–drag ratio K increases but without apparent change of lift, which means the effect of bi–flap–system on reducing drag is more prominent than that with single LEF. By changing the value of n,an optimum plan–form of the wing–1 can be found.

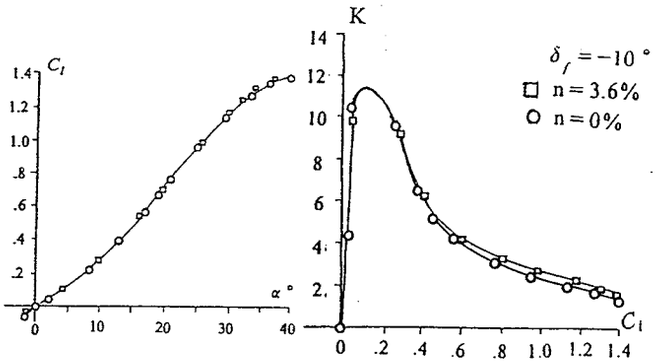

Fig.7 Characteristic K–C_l and C_l–α Curves of the Wing–1 with $\delta_f = -10$ ° for the ratio of apex–flap n = 0 and 3.6%

Aerodynamic effect of the bi–flap system on wing–2 and on wing with NASA patterned LEF

In this paragraph, the aerodynamic characteristics of the wing –2 (i.e. delta–wing equipped with out–stretched flaps having broken lined leading–edge) is to be discussed in comparison with that of the NASA wing (i.e. delta–wing equipped with the NASA patterned LEF) and the main wing (i.e. 74 ° swept delta–wing). The wing–planforms are as sketched in fig.1 with their geometrical parameters noted in Table 1.

Table 1 Geometrical parameters of wings (length unit: meter)

kind of model	root chord	mean aerody–namic chor	wing area	aspect tatio	span	area ratio of AF to wing,n	area ratio of LEVF to wing
delta–wing	0.592	0.395	0.100	1.160	0.340	7.4%	–
wing –2	0.592	0.380	0.130	1.520	0.444	5.8%	22.3%
NASA wing	0.592	0.447	0.134	1.160	0.394	–	23.7%

The aerodynamic C_n–α, C_a–α and K–α characteristic curves of the wing–2 (with AF deflection $\delta_f = -15$ °) and the NASA wing are drawn for $\delta_v = -30$ ° as shown in fig.8, where C_n and C_a are the coefficients of normal and tangential force with the negative signs denoting the downward and backward direction respectively. It is obvious that the wing–2 can keep the characteristics of normal force in same level as that of the NASA wing (Fig.8a) while having larger tangential force

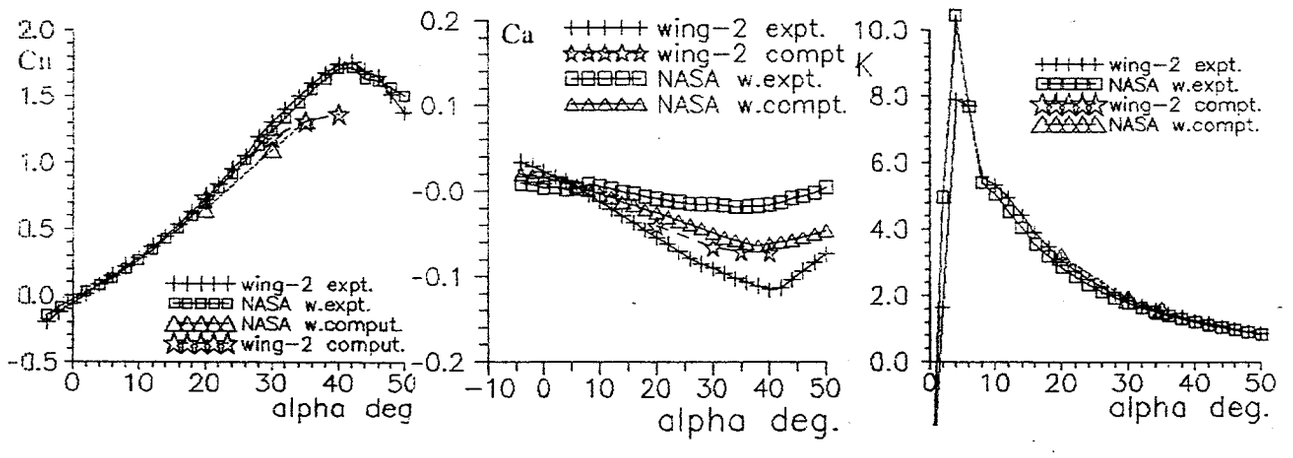

Fig.8 Characteristic C_n,C_a and K–α Curves of the NASA–Form wing and the Wing–2 with the Comparison of Computational and Experimental Results ($\delta_f = -15$ deg °)

xin

directing forwards (Fig.8b). This would be true, because the downward droop of the wing–2's apex–flap can bring an additional forwards directed force acting on the apex–flap with the decrease of normal force being compensated by the increase of normal force acting on the after part of the wing caused by the reduced downwash of flow passing around. Since C_l and C_d are obtained through the trasformation from C_n and C_a, the wing–2 can have its C_l larger and C_d smaller than that of the NASA wing at same AOA, resulting an increase of lift–drag ratio (Fig.8c). The superiority of wing–2 to NASA wing reflects the prominent merit of using bi–flap–system. By the way, correesponding computational curves representing the solution of N–S equations are drawn in Fig.8, which shows the tendency of variation agreeing well with that of the experimental curves. The computation for the numerical simulation is to be described in next paragraph. In Fig.9, the aerodynamic characteristic curves of wing–2 with $\delta_f=0$ ° and the NASA wing are drawn to compare with that of the main 74 ° swept delta–wing. In this case, the reduction of the drag of wing–2 is purely due to the effect of LEF since AF is not deflected(i.e. $\delta_f=0$ °). Moreover, here the mergence of the two separated vortices is delayed for the strength of AF vortex is now stronger than that in the case of $\delta_f=-15$ ° . The delayed mergence will weaken the effect of vortex interaction and the corresponding ability of reducing drag,which can be verified by the fact that the declination of the tangential force coefficient Ca vs. AOA of the wing–2 with $\delta_f=0$ ° is less steeper as shown in fig.9b than its counterpart with $\delta_f=-15$ ° (Fig.8b), but is still steeper than that of the NASA wing(Fig.9b). In addition, as it can be found in Fig.9a, although there are reduction of α_{cr} and C_{lmax} as the downward drooped angle of AF is to decrease from $\delta_f=-15$ ° to 0 ° in comparison with that of the NASA wing (however still much greater than that of the pure delta–wing), the normal force coefficient C_n is comparable to that of the pure delta–wing and larger than that of the NASA wing in the medium AOA range (Fig.9a). This verifies another superiority of wing–2 to NASA wing in enhancing the normal force and in turn the increase of lift. Herewith appears the C_d of wing–2 at $\delta_f=0$ ° smaller than that of NASA wing at the same C_l, while both are less than the corresponding C_d of the pure delta–wing (Fig.9c). All these have proved the fact that the bi–flap control has advantageous effects on reducing drag and enhancing the lift–drag ratio of the sweptback wing even when $\delta_f=0$ ° .

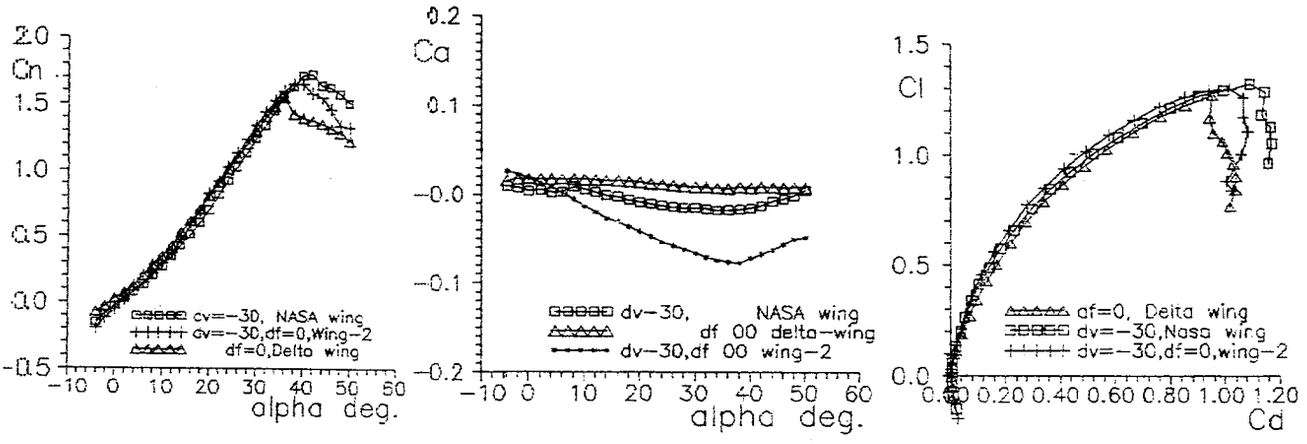

Fig.9 Characteristic C_n, C_a vs. α and C_l–C_d Curves of the Delta–Wing, Wing–2 and NASA–Form Wing

Numerical simulation of the action of bi–flap–system on vortex control

The numerical simulation was carried out by computation using the pseudo–compressibility method in solving the 3–D Navier–Stokes equations which can be expressed in conservative form as:

xin

$$\frac{\partial \hat{Q}}{\partial \tau}+\frac{\partial(\hat{E}-\hat{E}_v)}{\partial \xi}+\frac{\partial(\hat{F}-\hat{F}_v)}{\partial \eta}+\frac{\partial(\hat{G}-\hat{G}_v)}{\partial \zeta}=0. \tag{1}$$

$$\hat{Q}=\frac{1}{J}\begin{bmatrix} p/\beta \\ u \\ v \\ w \end{bmatrix},\hat{E}=\frac{1}{J}\begin{bmatrix} U \\ Uu+\xi_x p \\ Uv+\xi_y p \\ Uw+\xi_z p \end{bmatrix},$$

$$\hat{F}=\frac{1}{J}\begin{bmatrix} V \\ Vu+\eta_x p \\ Vv+\eta_y p \\ Vw+\eta_z p \end{bmatrix},\hat{G}=\frac{1}{J}\begin{bmatrix} W \\ Wu+\zeta_x p \\ Wv+\zeta_y p \\ Ww+\zeta_z p \end{bmatrix}. \tag{2}$$

Here, β is the pseudo-compressibility factor, J the Jacobian of the transformation (referring to[15] for detail). In discretization, the Euler backward difference to the time-derivative was applied. After completing the linearization with regard to the previous time step, an equation of implicit delta form was obtained. By using an approximately factorized implicit scheme of Beam-Warming type, the above equation can be expressed as:

$$L_\xi L_\eta L_\zeta(\hat{Q}^{n+1}-\hat{Q}^n)=RHS^n. \tag{3}$$

where L_ξ, L_η, L_ζ are operators, whose expressions can be found in related references[15] and therefore are omitted here. The spatial derivatives in the left-hand side are discretized in central difference, however for the terms in right-hand side, the spatial derivatives of the inviscid term are approximated with the TVD scheme[16] shown as follows:

$$RHS^n=-\Delta\tau\left[(D_\xi\hat{E}+D_\eta\hat{F}+D_\zeta\hat{G})-(\delta_\xi\hat{E}_v+\delta_\eta\hat{F}_v+\delta_\zeta\hat{G}_v)\right]^n \tag{4}$$

$$D_\xi\hat{E}=\tilde{E}_{i+1/2}-\tilde{E}_{i-1/2} \tag{5}$$

where the numerical flux is defined as:

$$\tilde{E}_{i+1/2}=\frac{1}{2}\left[\hat{E}_i+\hat{E}_{i+1}+\frac{R_{i+1/2}\Phi_{i+1/2}}{J_{i+1/2}}\right]. \tag{6}$$

Here $R_{i+1/2}$ is a matrix whose column vectors are the right eigenvectors of the flux Jacobian $\hat{A}=\partial\hat{E}/\partial\hat{Q}$ evaluated at some symmetric average of $\hat{Q}_i$ and $\hat{Q}_{i+1}$. We take an arithmatic average because of the incompressibility and use the Harten-Yee seconder-order upwind TVD scheme. Free-stream condition is specified at the upstream inlet ($i=1$) and the farfield boundary ($k=k_{max}$). At the downstream exit plane, the pressure is fixed to free-stream value and velocity components are linearly extrapolated from the interior points. Symmetry conditions are enforced on the symmetry planes ($j=1$ and $j=j_{max}$). On the wing surface no-slip condition $u=v=w=0$ and zero normal pressure gradient $\partial p/\partial n=0$ are used. Behind the trailing-edge, the flow variables on the surface $k=1$ are obtained by averaging the values extrapolated from the upper and lower interior points.

An H-O grid for computation is obtained by stacking along the streamwise ξ direction the two-dimensional grid generated in the cross-section plane. In each cross-section plane, a body-fitted "O" type grid is generated by using a parabolic procedure, marching from $k=1$ to the outer boundary.

Because the flow field is symmetric with respect to the x-z plane, only half flow-field needs to be computed. The grid size is $51(\zeta)\times51(\eta)\times49(\xi)$. The computational domain extends 1.0 and 1.5 root-chord length to the upstream and downstream respectively and extends 2 root-chord length from the x-axis to the outer boundary. Grid clustering is used in ζ (normal) direction with a minimum spacing 7×10^{-5} at the wing apex edge. About half of the grid points in the ξ direction are placed on the wing surface. Fig.10 shows the sketch of the cross-plane grid.

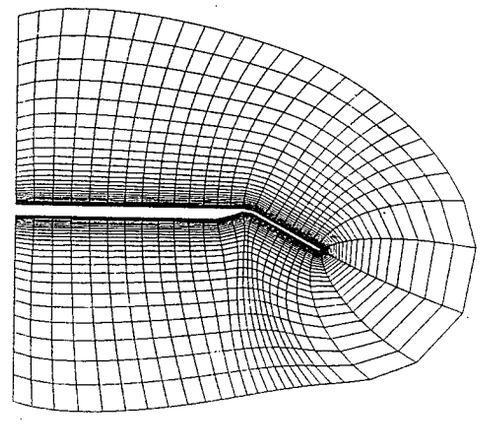

Fig.10 The Sketch of the Sectional Grid.

For laminar flow, as we had computed for $Re=1\times10^4$ and described in[10][18], we used two schemes in discretizing the spatial derivatives: one was the central difference scheme which requires the artificial viscosity terms added to make the computation stable; the other was the upwind compact difference scheme which was more accurate since no artificial dissipation was needed. Through comparison between the computational and experimental results, it seemed that although the lift-drag ratio K vs. α

xin

curves can fit better with each other, however the C_l and C_a vs. α curves can fit well only for a < 25 ° . There are lower computational valus of C_{lmax} and α_{cr} which may be due to the effect of lower computational Re number and without taking the turburence into consideration. As concerns this matter, now we borrow the second order total variation diminishing(TVD) scheme of Harten–Yee type[16] from the compressible flow to compute the flow for $Re = 1 \times 10^6$ and taking the effect of turbulence into consideration preliminarily by employing the algebraic turbulence model of Baldwin–Lomax. Here the description about the Baldwin–Lomax model of turbulence is omitted too, since it is a quite wellknown model having the advantage of requiring less information about the edge of boundary layer.

In turbulent flow computation, the viscosity ν is, presumably, a sum of the coefficients of laminar flow and turbulent flow, i.e. $\nu = \nu_l + \nu_t$. The field of turbulent flow is divided into inner and outer regions with different set of equations used in each region to determine the turbulent viscosity ν_t. Curves in fig.11 are to show the comparison for $Re = 1 \times 10^6$ between the experimental results and the computational results obtained by solving the Navier– Stokes equations with the influence of turbulence considered preliminarily by the Baldwin–Lomax model. Here the agreement is better than that comparing with the computation of laminar flow in lower $Re = 1 \times 10^4$ as we had done and described in Ref.10.

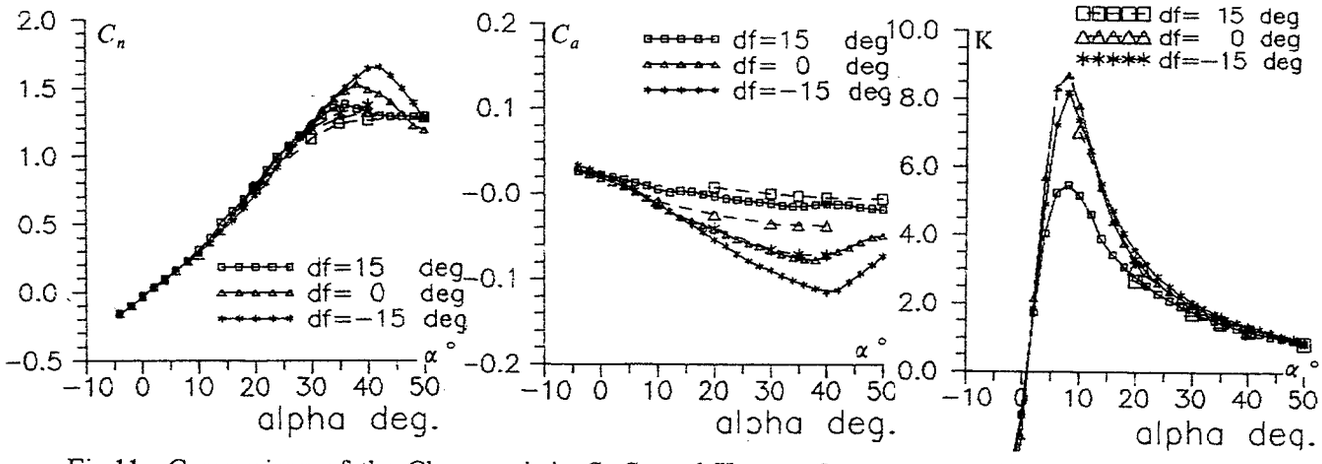

Fig.11 Comparison of the Characteristic C_n,C_a and K vs. α Curves of the Wing–2 between the N–S Computation and Experiment

Effects of Using Bi–Flap–System on the Vortex Control in High Speed and Wing–Body Case

The effect of using bi–flap–system on vortex control can appear in high speed up to $Ma = 2$[6] and in the case of wing–body combination[18] as we have studied before. Taking the lift–drag ratio K of the 74 ° swept delta–wing for example, the experimental curves showing the variation of K vs. C_l for $Ma = 0.8$ and 2.01 (Fig.12) as well as for that of double delta wing–body combination(Fig.13) with its planform shown in Fig.14 are depicted. It is apparent that K for compressible flow and in the case of wing–body combination are to increase by drooping down the AF($\delta_f < 0$) at constant AOA similar to that in low speed and pure wing respectively.

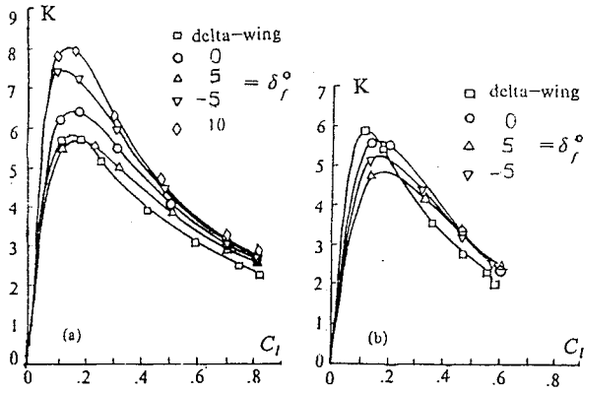

Fig.12 Characteristic K–C_l Curves of the Wing–1

(a) Ma = 0.8, (b) Ma = 2.01

Xin

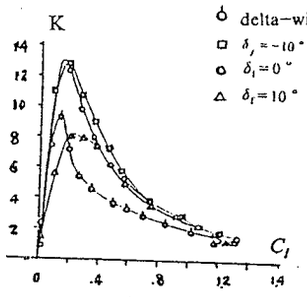

Fig.13 Characteristic K–C_l Curve of the Double Delta–Wing Body Combination

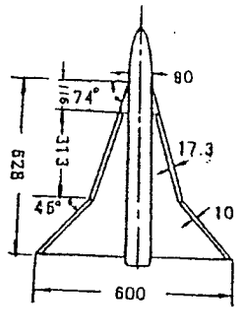

Fig.14 Planform of the double delta–wing body combination (length unit:mm)

Conclusions

The effectiveness of using bi–flap–system on improving the caracteristics of sweptback wing is verified to be superior to single flap by experiments and the computation through solving the Navior–Stokes equations.

By controlling the deflection of flaps, the aerodynamic improvements such as lift–rise, drag reduction, delay of vortex break–down and the increase of maximum lift coefficient and critical AOA can be achieved, in which the vortex interaction in lowing the rate of decay of vortex strength and promoting the mergence of separated vorteices play an important role. The superiority of using bi–flap–system appears also in high speed range up to Ma=2 and in the case of wing–body combination. It is our purpose that the promising vortex–control technique can be extended to practical use and to improve the performance of aircrafts in aeronautical and astronautical fields in future.

Acknoledgments.

The first auther would like to express thanks to his colleagues and graduate students whose names appear in the references for their help and contribution to this work.

References

1 Rao,D.M.,Campell,J.F.:Vortical flow management techniques,Prog.Aerospace Sci. vol.24,1987,pp173–224.

2 Rao,D.M.:Leading–edge vortex–flap experiments on a 74 ° delta wing,NASA CR–159161,No .1979.

3 Lamar,J.E.,Campbell,J.F.:Recent studies at NASA–Langley of vortical flows interacting with neighboring surfaces, Paper No.10, AGARD fluid dynamics panel symposium on vortical type flows in three dimensions, April 1984.

4 Zhuang,F.G.,Hsing,T.D.,Wang,Z.F.,Zhang ,Z.J.,Kuo,W.H.:Aerodynamic characteristics of the vortex flap and its combination with apex flap,ACTC AERODYNAMICA SINICA, Vol.6 No.1,Mar.1988,pp81–91.

5 Hsing,T.D.,et.al.:Effectiveness of combination of apex– and leading–edge vortex flap on a 74 ° delta–wing with or without trailing–edge flap, ICAS–88–4.5.1, Jerusalem,Israel, August 1988.

6 Hsing,T.D.,Zhang,Z.Q.,et.al.:A study of the interaction of separated vortices in transonic and supersonic flow on improving the aerodynamic charateristics of vortex–flap, IUTAM symposium in Novosibirsk,Springer– Verlag,1990,pp.475–483.

7 Klute,S.M.,Rediniotis,O.K.,Telionis,D.P Flow control over a maneuvering delta wing at high angles of attack,AIAA J.,Vol.34, no.4,April 1996, pp662–668.

8 Lamar,J.E.,Campbell,J.F.:Vortex flap––advanced control devices for supercruise fighters, Aerospace America, Vol.22, Jan.1984,pp95–99.

9 Hsing,T.D.:Vortex control over sweptback wing and a model study of control– configuration–vehicle, Collection of Treatises on Aerodynamics in Advance, Publisher of Defence Industry, 1997, pp95–122.

10 Hsing,T.D.,Yu,G.Z.,Gu,Z.F.:Aerodynamic characteristics of a highly swept wing in steady / unsteady pitching states and effects of flap control at large incidence, Proc. of 20th Congress of ICAS, ICAS–96–2.10.5,Sorrento Italy, 1996, pp2278–2288.

11 Guo,W.H.:Vortex interaction and its influence on the aerodynamic characteristics of slender wings, Dissertation BUAA, June 1989.

Xin

12 Christiansen,J.P.,Numerical simulation of hydromechanics by the method of point vortices, J.Comput.phys.,vol.13,1973,pp363–379.

13 Tang,S.J.,Zhuang,F.G,Hsing,T.D.,Determi nistic vortex method for simulation of vortex interaction in two dimensional flows, Proc. First Sino–Soviet Workshop on Complex Fields of Gas Flow, Beijing, China, 1991.

14 Wang,W.G.,Zhuang,F.G.,Hsing,T.D.:The direct numerical simulation of three dimensional merger for two parallel vortex tubes, ACTA MECANICA SINICA, Vol.30 No.1,Jan.1998,pp1–8.

15 Kwak,D., et al.:An incompressible Navier–Stokes flow solver in three–dimensional curvilinear coordinates systems using primitive variables, AIAA Paper 84–0253,1984.

16 Yee,H.C.,A class of high–resolution explicit and implicit shoot–capturing methods, NASA TM 101088,1989.

17 Yu,L.,Hsing,T.D.:A Comparison of the experimental and computational study on the effects of vortex–control by deflecting flaps on a highly swept delta wing, ACTA AERONAUTICA ET ASTRONAUTICA SINICA – English edition, 1998,(to appear).

18 Hsing,T.D.,Zhang,Z.Q.,Zhuang,F.G.:The impact of apex–flap on vortex–flapped delta and double delta wings, AIAA Paper 91–3218, 1991.

Xin